



Proximal magnetometry of monolayers of magnetic moments

Z. Salman^{a,*}, S. J. Blundell^b

^aLaboratory for Muon Spin Spectroscopy, Paul Scherrer Institut, CH-5232 Villigen PSI, Switzerland

^bClarendon Laboratory, Department of Physics, Oxford University, Parks Road, Oxford OX1 3PU, UK

Abstract

We present a method to measure the magnetic properties of monolayers and ultra-thin films of magnetic material. The method is based on low energy muon spin rotation and β -detected nuclear magnetic resonance measurements. A spin probe is used as a “proximal” magnetometer by implanting it in the substrate, just below the magnetic material. We calculate the expected magnetic field distribution sensed by the probe and discuss its temperature and implantation depth dependencies. This method is highly suitable for measuring the magnetic properties of monolayers of single molecule magnets, but can also be extended to ultra-thin magnetic films.

Keywords: Single molecule magnets, ultra-thin magnetic films, monolayer, proximal magnetometry

1. Introduction

Recent developments of low energy muon spin rotation (LE- μ SR) [1, 2] and β -detected nuclear magnetic resonance (β -NMR) [3, 4], provide unique local spin probe tools for measurements in thin films and multilayers. However, the application of these methods is limited by a minimal thickness of films, which provides sufficient stopping power for the implanted probes. For typical density materials a minimal 1-2 nm thickness is required at the lowest available implantation energy (1-2 keV). Therefore, these methods are generally not suitable for studies of monolayers and ultra-thin films. Nevertheless, for magnetic materials it is possible to perform a “proximal” measurement by implanting the probe in the substrate (or an under-layer) of the material, and sensing the dipolar magnetic fields from the layer of interest [5, 6].

To date, measurements of the magnetic properties of monolayers of single molecule magnets [7] (SMMs) have been mostly performed using X-ray absorption spectroscopy (XAS) and X-ray magnetic circular dichroism (XMCD) [8, 9]. These are typically limited to high magnetic fields and provide information regarding the average static magnetic properties of the irradiated portion of the monolayer. In contrast, LE- μ SR and β -NMR provide local probe measurements with important advantages; sensitivity to a large range of spin fluctuations and dynamics and applicability in zero or any applied magnetic field. However, a detailed interpretation of the measured spectra using LE- μ SR [6] or β -NMR [5] when implanting the probe just below the monolayer is still absent. In this paper we calculate the magnetic field distribution in a non-magnetic substrate due to a monolayer of SMMs. This distribution can be used to fit LE- μ SR and β -NMR measurements, providing information regarding the magnetic and geometric properties of the monolayer. The calculations can be easily generalized for the case of ultra-thin magnetic films by considering the domains as individual magnetic moments with a given average size.

*Tel. +41-56-310-5457

Email address: zaher.salman@psi.ch (Z. Salman)

2. Uniformly Magnetized Sheet Approximation

As a simple approximation, a monolayer of magnetic moments (or a thin film) can be viewed as a uniformly magnetized sheet. Assuming magnetic moment M per unit area, located in the plane $z = 0$ (see inset of Fig. 1) with the magnetization aligned along $-\hat{z}$. The magnetic scalar potential from an annular region of radius ρ and width $d\rho$ is

$$d\phi_M(\rho, z) = -\frac{Mz\rho d\rho}{2(z^2 + \rho^2)^{3/2}}. \quad (1)$$

The contribution of such a region to the magnetic field at a distance z from its center is

$$dB_z(\rho, z) = -\mu_0 \frac{\partial(d\phi_M)}{\partial z} = \frac{\mu_0 M}{2} \frac{\rho(\rho^2 - 2z^2)}{(\rho^2 + z^2)^{5/2}} d\rho, \quad (2)$$

where μ_0 is the permeability of the vacuum. We plot this contribution as a function of ρ/z in Fig. 1. Integrating the

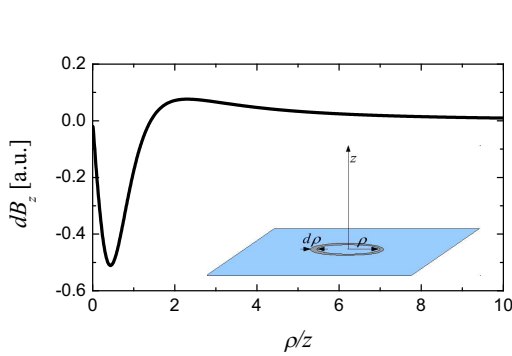


Figure 1: The contribution dB_z of one annular region as a function of ρ/z . The inset shows a uniformly magnetized sheet divided into annular regions.

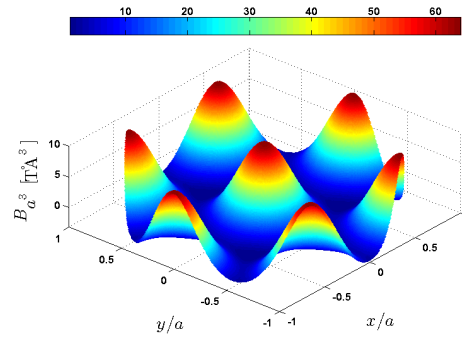


Figure 2: The z component of the field, sensed by a spin probe at $z = a/2$, as a function of position. The color scale represents the strength of the field.

contributions from all annuli gives a magnetic field zero as expected.

However, this approximation fails when looking at the microscopic structure of the sheet, i.e., as a collection of individual magnetic moments or even randomly oriented magnetic domains. This is the case when measuring the field due to such sheet using a local spin probe, which is positioned at a distance smaller than the microscopic details of the sheet (distance between moments or size of domains). For example, if we have a monolayer of moments with average spacing a between them, then the magnetic field sensed by a spin probe at a distance $z < a$ from the monolayer is non-zero.

3. Monolayer of Magnetic Moments

In order to adequately account for the microscopic structure of a monolayer of magnetic moments, $\vec{\mu}_i$, one needs to sum the contribution of all moments in the monolayer. The dipolar field from $\vec{\mu}_i$ at $\vec{r}_i = x_i\hat{x} + y_i\hat{y} + z_i\hat{z}$ is

$$\vec{B}_i(\vec{r}_i) = \frac{\mu_0}{4\pi} \frac{3\vec{r}_i(\vec{\mu}_i \cdot \vec{r}_i) - \mu_i^2 \vec{r}_i}{r_i^5}. \quad (3)$$

A typical NMR or transverse field μ SR measurement is sensitive to the field distribution of one component of the field. In what follows we will restrict ourselves to the B_z component, where z is normal to the monolayer surface. Working in polar coordinates with $\vec{\mu}_i = \mu_\rho^i \hat{\rho} + \mu_z^i \hat{z}$ and $\vec{r}_i = \rho_i \hat{\rho} + z_i \hat{z}$ we can write

$$B_z^i(\rho_i, z_i) = \frac{\mu_0}{4\pi} \frac{3z_i \rho_i \mu_\rho^i + 2z_i^2 \mu_z^i - \rho_i^2 \mu_z^i}{(\rho_i^2 + z_i^2)^{5/2}}. \quad (4)$$

Therefore the field distribution, $n(z, B)$, can be obtained by summing the contribution from all magnetic moments. For simplicity, we start by considering a monolayer of moments $\vec{\mu}_i = \mu\hat{z}$ in the plane $z = 0$, arranged on a triangular lattice with lattice constant a . For example, taking $\mu = \mu_B$, a spin probe at $z = a/2$ will sense dipolar fields as shown in Fig. 2. The resulting field distribution is shown in Fig. 3(a), where different curves are results of summation of a different number of moments, such that N is the radius (in units of a) of the considered “patch”. In order to sample a field distribution as in Fig. 2, it is sufficient to sample only a unit cell of an equilateral (a) triangular area between 3 moments¹. Note that the qualitative shape of the distribution is almost independent of N . However, due to the finite number of considered moments, we find a strong shift which decreases as a function of N .

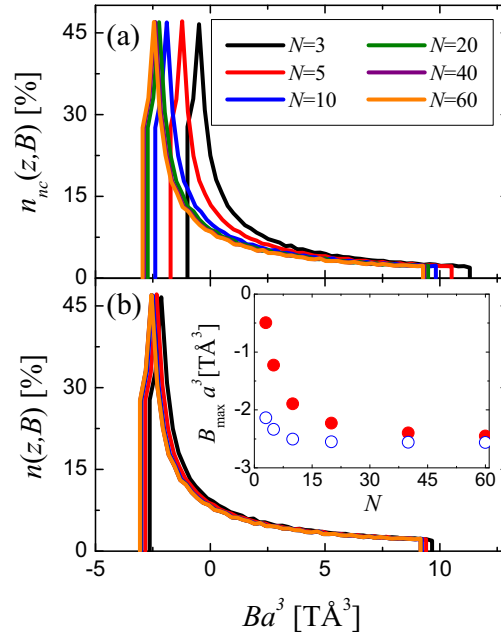


Figure 3: The distribution of B_z sensed by a spin probe due to a patch of moments with radius N (a) before and (b) after the correction in Eq. 6. The inset shows the most probable field as a function of N before (full symbols) and after (empty symbols) correction.

In order to correct for this “artifact” we need to account for all the moments in the infinite monolayer. However, since the moments outside the patch satisfy the criterion of a uniformly magnetized sheet, i.e. $r_i \gg a$, their contribution can be calculated as an infinite sheet of uniform magnetization with a hole of radius $\rho_0 = aN$ around the origin. This can be calculated by integrating dB_z (Eq. 2) between $\rho = \rho_0$ and infinity,

$$\Delta B_z = \int_{\rho_0}^{\infty} dB_z(\rho, z) = \frac{\mu_0 M}{2\rho_0(1 + \zeta^2)^{3/2}}, \quad (5)$$

with $\zeta = z/\rho_0$. In contrast to the case of a uniformly magnetized sheet, ΔB_z here does not vanish for finite ρ_0 . Note that when the spin probe is far from the monolayer, such that $\rho_0 \gg z$, then $\Delta B_z \approx \frac{\mu_0 M}{2\rho_0}$. This is quite different from the three dimensional case, where the remaining contribution is $\frac{\mu_0 M}{3}$ (where in this case M is the three-dimensional magnetization, i.e. the magnetic moment per unit volume), independent of how far we integrate out to.

Assuming uniform magnetization due to moments $\mu = \mu_B$, ordered on a triangular lattice with lattice constant a , the magnetic moment per unit area is $M = \mu_B/(\sqrt{3}a^2/4)$. Using $N = \rho_0/a$ we arrive at,

$$\Delta B_z = \frac{2\mu_0\mu_B}{\sqrt{3}a^3N(1 + \zeta^2)^{3/2}}. \quad (6)$$

¹Due to the symmetry of the lattice the sampling can also be done on 1/6 of this area

This is the cause of shift seen in Fig. 3(a), and should be subtracted from the dipolar field of the patch of moments to correct for its finite size effect. Comparison between the field distribution before (Fig. 3(a)) and after (Fig. 3(b)) the correction shows clearly how well it works. Taking into consideration a patch with $N = 10$ is already sufficient to accurately calculate the field distribution. Note that without the correction, even a patch with $N = 60$ exhibits a small artificial shift (inset of Fig. 3).

The field distribution has a similar shape to that in the vortex state of a superconductor [10]. The high field cut-off is due to probes stopping exactly below a magnetic moment, while the low field cusp is due to probes stopping in middle between three neighbouring moments. However, one important difference between this case and a vortex lattice is that in the former the field distribution depends strongly on the stopping depth of the probe while in a superconductor the depth dependence is much weaker [11, 12]. As we show below, this strong depth dependence will alter the shape of the field distribution entirely in a real measurement. Nevertheless, it is important to point out here that the shape of $n(z, B)$ is determined by the lattice constant a and the size of magnetic moment μ . Hence, these parameters can, in principle, be extracted directly from a measurement of the field distribution. Also, the details of the lattice, e.g. triangular or other, do not alter the qualitative shape of $n(z, B)$ dramatically.

4. Measured Field Distribution

In a LE- μ SR or β -NMR measurements, the implanted probes stop in the sample at a distribution of depths, $D(z)$, rather than a unique single depth. This distribution can be simulated accurately [13, 14] using Trim.SP Monte-Carlo code [15]. Therefore, the calculated $n(z, B)$ should be averaged over $D(z)$. Moreover, since the probe stops in the substrate of the monolayer, its intrinsic line shape (field distribution) has to be convoluted with the depth averaged field distribution. Finally, disorder in the monolayer, e.g. deviations from a perfect triangular lattice, can be taken into account by convoluting the depth averaged distribution with a Gaussian of width that represents the degree of disorder. In practice, one can simply convolute the calculated distribution with a single Gaussian or Lorentzian that includes both substrate and disorder effects. The resulting field distribution is then

$$L(B) = I(B) * \int_{z_0}^{\infty} D(z)n(z, B)dz, \quad (7)$$

where $I(B)$ is the broadening due to the substrate and disorder, and z_0 is the distance between the magnetic cores in the monolayer and the surface of the substrate. In the case of SMMs, z_0 is due to the ligands used to graft the magnetic core of a SMM to the substrate. In Fig. 4, we plot a typical field distribution due to a monolayer of $1\mu_B$ moments, with $a \sim 5$ nm, $z_0 \sim 1$ nm and a stopping profile as shown in the inset. Both, the distribution with (solid line) and

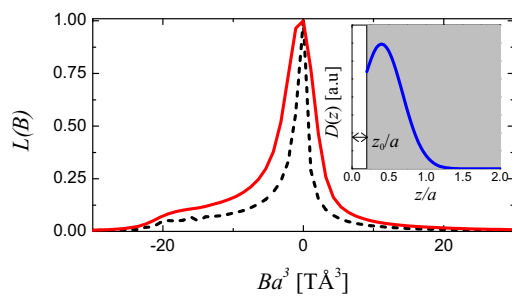


Figure 4: The field distribution $L(B)$ sensed by a spin probe due to a monolayer of moments at $z = 0$. The dashed and solid lines are calculated with and without broadening, respectively. The inset shows a typical stopping profile of implanted probes in the substrate (shaded area).

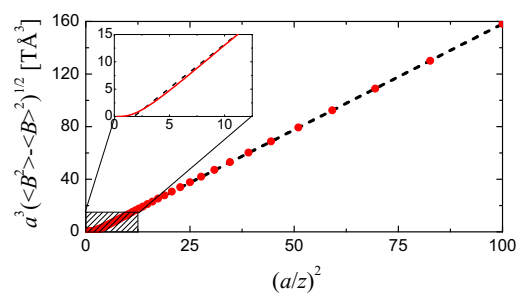


Figure 5: The square root of the second moment of the field distribution as a function of distance from the monolayer (circles and solid line in inset). The inset is an expanded view of the shaded area. The dashed line is the fit described in the text.

without (dashed line) the broadening $I(B)$ are shown. Surprisingly, the asymmetry of the distribution after averaging over depth is opposite to that of a single depth, i.e. we find a low field instead of the high field tail in Fig. 3. This is due to a larger near-zero field contribution of probes implanted deeper into the substrate, far away from the magnetic

cores in the monolayer. Note that unlike Fig. 3, the most probable field in $L(B)$ is much closer to $B = 0$, and therefore in a real measurement we do not expect to see a considerable shift in the precession frequency of the probe, instead only some broadening can be measured [5, 6].

Now we turn to the depth dependence of the field distribution. As we mentioned earlier, we expect that for a depth $z \gg a$ the dipolar field of the magnetic moment vanishes as in the case of a uniformly magnetized infinite sheet. The depth dependence can be very useful in measurements as a tool for identifying (I) the nature of the sensed magnetic fields by the probe, dipolar or other, and (II) to estimate the characteristic length scale, a , in the monolayer [5]. In Fig. 5 we plot the second moment of the field distribution as a function of depth. The dashed line is a linear fit of the second moment as a function of $(a/z)^2$ in the range 50–100. Clearly, the second moment is inversely proportional to z^2 . This is in contrast to the $1/z^3$ dependence of the dipolar field from a single moment. A very small deviation from the $(a/z)^2$ behaviour can be seen for $z \geq a/3$ (see inset of Fig. 5). Note also that the second moment vanishes at $z \sim a$, as expected.

5. Information Drawn from an Experiment

Considering actual measurements, in LE- μ SR we measure the time dependence of the polarization of the implanted muons in an applied transverse field. This is proportional to the Fourier transform of field distribution sensed by the muons, so that the average precession frequency is proportional to the average field and damping rate is proportional to the width of field distribution. In a β -NMR experiment we measure the ^8Li nuclear magnetic resonance line which directly proportional to the field distribution. In both cases it is, in principle, possible to fit the measured spectra. However, the asymmetry of the field distribution is quite small, and therefore hard to detect within the uncertainty of the measurement. Usually it is sufficient to approximately fit the data assuming a simple Lorentzian field distribution. As we mentioned above, there is no detectable shift in the average field as a function of depth and temperature. In contrast, the width of the distribution depends strongly on these parameters. In fact, the width is proportional to $\langle \mu^2 \rangle$. Therefore, its temperature dependence can be obtained by measuring the temperature dependence of the field distribution width at a fixed depth (implantation energy). From this one should subtract the additional broadening due to the substrate. This can be easily evaluated by a measurement of the field distribution as a function of temperature dependence at large depths (high implantation energy). Finally, we point out that since we are dealing with local probe measurements, the averaging in $\langle \mu^2 \rangle$, is on individual moments during the lifetime of the probe. This is different from the case of a XMCD measurement, where the averaging is done on the absorption signal from all molecules.

6. Conclusions

We have presented a detailed calculation of the properties of the magnetic field distribution, measured in the substrate, due to a monolayer near its surface. This distribution and its depth dependence can be used to infer the properties of the monolayer, such as the size of magnetic moment and the average distance between neighbouring moments. Although we restricted our calculations to oriented moments on a triangular lattice, they can be easily generalized for different systems. Nevertheless, the depth dependence of the width of the distribution (i.e. relaxation rate of the muon spin precession) and its temperature and depth dependencies should not be affected by the geometric details of the lattice.

References

- [1] E. Morenzoni et al., Phys. Rev. Lett. 72 (1994) 2793.
- [2] T. Prokscha et al., Nucl. Instr. and Meth. A 595 (2) (2008) 317–331.
- [3] Z. Salman, E. P. Reynard, W. A. MacFarlane, K. H. Chow, J. Chakhalian, S. R. Kreitzman, S. Daviel, C. D. P. Levy, R. Poutissou, R. F. Kiefl, Phys. Rev. B 70 (2004) 104404.
- [4] G. D. Morris et al., Phys. Rev. Lett. 93 (2004) 157601.
- [5] Z. Salman et al., Nano Lett. 7 (2007) 1551.
- [6] Z. Salman et al., arXiv:0909.4634v1.
- [7] D. Gatteschi, R. Sessoli, J. Villain, Molecular Nanomagnets, Oxford University Press, 2006.
- [8] M. Mannini et al., Nature Mater. 8 (3) (2009) 194–197.
- [9] M. Mannini et al., Nature 468 (7322) (2010) 417–421.

- [10] E. H. Brandt, *J. Low. Temp. Phys.* 73 (5-6) (1988) 355–390.
- [11] C. Niedermayer et al., *Phys. Rev. Lett.* 83 (1999) 3932.
- [12] Z. Salman et al., *Phys. Rev. Lett.* 98 (2007) 167001.
- [13] E. Morenzoni et al., *Nuc. Inst. Meth. Phys.* 192 (2002) 254.
- [14] T. A. Keeler et al., *Phys. Rev. B* 77 (14) (2008) 144429.
- [15] W. Eckstein, *Computer Simulation of Ion-Solid Interactions*, Springer, Berlin, Heidelberg, New York, 1991.